Supporting Information

Iron hydroperoxide intermediate in Superoxide Reductase: Protonation or Dissociation First? MM Dynamics and QM/MM Metadynamics study.

Rolf David, [†,‡,§] *Hélène Jamet,* [†,‡] *Vincent Nivière,* [‖] *Yohann Moreau,* [§] *Anne Milet* *[,†,‡]

†Univ. Grenoble Alpes, DCM, F-38000 Grenoble, France

‡ CNRS, DCM, F-38000, Grenoble, France

§ Laboratoire de Chimie et Biologie des Métaux, CEA/DRF/BIG/CBM/MCT, CNRS UMR 5249, Université Grenoble Alpes, Grenoble, France

‖ Laboratoire de Chimie et Biologie des Métaux, CEA/DRF/BIG/CBM/BioCat, CNRS UMR 5249, Université Grenoble Alpes, Grenoble, France

*To whom correspondence should be addressed: anne.milet@univ-grenoble-alpes.fr

I. Computational details and methods

1. Cartesians coordinates for small and large models used for deriving MM parameters.

Small Model – DX Active Site

Fe	-0.20753	-0.26356	0.37835
S	0.10198	-2.27411	-0.73420
S	1.37464	0.31883	1.97616
S	-2.17492	-0.40073	1.57532
S	-0.22093	1.30246	-1.34140
C	2.85287	-2.45015	-1.31723
C	3.81051	0.66861	0.57021
C	-3.92887	-0.63657	-0.63948
C	-0.69449	4.03964	-1.56678
C	1.52803	-1.91497	-1.85895
C	2.63780	1.42420	1.19971
C	-3.30072	-1.41918	0.51382
C	-0.72285	2.89480	-0.55141
H	3.05166	-2.06264	-0.31472
H	2.82936	-3.54520	-1.24769
H	3.68884	-2.16690	-1.97595
H	4.26374	-0.02683	1.28662
H	3.47968	0.09537	-0.29919
H	4.58705	1.37432	0.23447
H	-4.50906	0.21597	-0.26488
H	-3.15580	-0.24982	-1.31158
H	-4.60336	-1.28382	-1.22176
H	0.31286	4.17376	-1.97945
H	-1.37351	3.83734	-2.40388
H	-1.00172	4.98589	-1.09602
H	1.29998	-2.37594	-2.82809
H	1.58842	-0.83485	-2.02503
H	2.15122	2.04858	0.44372
H	3.00325	2.08337	1.99745
H	-2.74118	-2.27619	0.12588
H	-4.08176	-1.80788	1.17973
H	-1.72926	2.77419	-0.13632
H	-0.05062	3.11253	0.28614

Large Model – DX Active Site

Fe	-0.42847	-0.97641	-1.46032
S	-1.14892	-3.02514	-0.51291
S	-1.95551	0.30798	-2.71421
S	1.21154	-1.33951	-2.87332
S	0.23004	0.33823	0.29969
O	-3.97671	-2.61604	2.94654
O	-3.37908	0.16462	1.24307
O	-5.69512	2.87198	-2.06103
O	4.79938	-2.01733	-2.95127
O	4.13982	-3.44609	1.14569
O	4.76553	-0.79365	3.44165
O	3.54855	1.40679	0.53183
O	1.71506	5.31776	1.51216
N	-5.70517	-1.93247	1.68139
N	-3.86075	-1.36399	-0.33172
N	-4.65313	2.07778	-0.22779
N	4.33387	-0.44522	-1.42477
N	2.69199	-2.14815	0.03019
N	2.67100	-0.73029	2.64510
N	2.69156	2.01029	2.51391
N	2.21568	3.87093	-0.14685
C	-6.63544	-1.74886	2.78764
C	-4.45945	-2.35556	1.84752
C	-2.15465	-2.61007	0.91136
C	-3.63916	-2.49363	0.56807
C	-3.70708	-0.11217	0.08749
C	-2.66764	1.48102	-1.55146
C	-3.97811	0.99386	-0.93036
C	-5.47414	2.91624	-0.84944
C	-6.14805	3.95883	0.03176
C	5.29429	0.47379	-2.00907
C	4.18639	-1.65328	-1.94864
C	2.01290	-2.83496	-2.23388
C	3.18335	-2.58558	-1.27547
C	3.21010	-2.64566	1.15021
C	2.62303	-2.17307	2.47634
C	3.76474	-0.15559	3.12855
C	3.74166	1.35362	3.27624
C	2.69175	1.99117	1.18805
C	0.89160	1.81572	-0.50978
C	1.56300	2.74329	0.49961
C	2.26562	5.06464	0.43552
C	3.04487	6.13312	-0.31090
H	-6.14346	-2.01148	3.72415

H	-7.50484	-2.39011	2.64215
H	-6.95492	-0.70742	2.82533
H	-6.04433	-1.72234	0.75352
H	-2.01424	-3.39076	1.65892
H	-1.79721	-1.65965	1.30773
H	-3.96691	-3.41378	0.08437
H	-4.13513	-1.54327	-1.28701
H	-1.93300	1.65100	-0.76435
H	-2.84428	2.41196	-2.09012
H	-4.61823	0.62562	-1.73199
H	-4.48267	2.18354	0.76209
H	-5.37629	4.56163	0.51049
H	-6.73238	3.44476	0.79492
H	-6.80249	4.60407	-0.55426
H	5.78859	-0.00522	-2.85427
H	6.03837	0.74683	-1.26083
H	4.77798	1.37062	-2.35137
H	3.77908	-0.17347	-0.62572
H	1.23950	-3.40789	-1.72235
H	2.36519	-3.39411	-3.10071
H	3.68255	-3.54910	-1.17227
H	1.95251	-1.46204	0.08074
H	1.58703	-2.50964	2.51465
H	3.18983	-2.65183	3.27486
H	1.87398	-0.16231	2.39550
H	3.61062	1.56918	4.33667
H	4.71378	1.72201	2.94855
H	1.95184	2.48765	3.00891
H	1.61986	1.50512	-1.25895
H	0.07105	2.34179	-0.99763
H	0.82534	3.11012	1.21333
H	2.63675	3.73750	-1.05513
H	2.59080	6.27413	-1.29174
H	4.07326	5.79306	-0.43270
H	3.03597	7.07750	0.23327

Small Model – SOR-superoxo Active Site

Fe	-0.37721	-0.33697	-0.15998
S	-0.96214	-0.36224	2.26181
O	0.10818	0.02502	-2.28084
O	-0.73032	-0.18793	-3.29562
N	3.66539	-1.63604	-1.30378
N	1.75341	-1.20409	-0.29228
N	1.65032	3.39155	1.01109
N	0.72077	1.62622	0.07670

N	-3.75137	2.19363	-1.46500
N	-2.32666	0.77694	-0.55816
N	-1.26434	-2.32611	-0.85352
N	-2.54769	-3.54352	-2.17321
C	5.40362	-1.20829	0.50036
C	3.99531	-1.33201	0.01004
C	2.31234	-1.54480	-1.43826
C	2.78917	-1.07329	0.61224
C	3.27750	4.21197	-0.75869
C	2.25762	3.25462	-0.23114
C	0.73705	2.38825	1.15192
C	1.65556	2.15538	-0.79053
C	-5.44316	2.62344	0.37910
C	-4.21600	1.96645	-0.17589
C	-2.61600	1.46224	-1.64884
C	-3.31404	1.08269	0.36305
C	0.46899	-0.70465	3.37468
C	0.08641	-4.14360	0.31323
C	-0.94650	-3.66867	-0.66471
C	-2.22175	-2.29236	-1.76330
C	-1.73994	-4.43320	-1.48483
C	6.04273	0.14750	0.13998
C	2.66417	5.53674	-1.24061
C	-5.67533	2.28235	1.85593
C	0.04023	-0.81784	4.84168
C	-0.35560	-4.01028	1.77902
H	6.02098	-2.02701	0.10366
H	5.39950	-1.33047	1.58982
H	4.31341	-1.87798	-2.04097
H	1.78671	-1.69576	-2.36899
H	2.60563	-0.78704	1.63693
H	3.79767	3.72654	-1.59265
H	4.04376	4.41441	0.00427
H	1.85603	4.10040	1.70159
H	0.12298	2.22606	2.02801
H	1.81528	1.70675	-1.76082
H	-6.32705	2.32547	-0.20586
H	-5.36098	3.71563	0.26819
H	-4.17586	2.80020	-2.15316
H	-2.05136	1.43049	-2.56977
H	-3.29043	0.65955	1.35638
H	1.21446	0.09806	3.27586
H	0.95786	-1.63847	3.07130
H	1.00666	-3.57086	0.16245
H	0.32031	-5.19264	0.08614
H	-2.65326	-1.39575	-2.17761

H	-3.22852	-3.77397	-2.88253
H	-1.80477	-5.50155	-1.62896
H	7.06774	0.20995	0.52589
H	5.46167	0.97228	0.56591
H	6.08275	0.29480	-0.94605
H	3.43866	6.20845	-1.63127
H	2.14824	6.06057	-0.42648
H	1.93262	5.35689	-2.03583
H	-6.57575	2.78412	2.22723
H	-4.82840	2.60043	2.47348
H	-5.80707	1.20405	1.99790
H	0.90666	-1.01774	5.48988
H	-0.68273	-1.63109	4.97170
H	-0.43880	0.10809	5.18172
H	0.46097	-4.29866	2.45347
H	-1.21116	-4.66584	1.98795
H	-0.65879	-2.98407	2.00405

Large Model – SOR-superoxo Active Site

Fe	0.27206	0.07620	-1.57032
S	1.78507	0.73762	0.43573
O	-1.16681	-0.44303	-4.28772
O	-0.89039	-0.92865	-3.07334
O	0.95453	6.42647	-0.98368
O	4.87672	4.43831	-1.92950
O	3.49213	3.58118	2.38221
O	1.10070	1.89644	5.65862
O	2.98627	-5.21454	1.01844
O	7.40538	-3.23781	-0.24782
O	-3.26064	-6.00629	1.76715
O	-5.94318	-5.84001	-0.75079
O	-5.86567	3.71374	2.36663
O	-5.45125	-0.20801	0.27789
N	2.44589	5.67609	0.53599
N	1.79454	1.94552	-5.15709
N	1.14226	1.44191	-3.11531
N	3.05980	3.40051	-1.07047
N	4.10098	1.50100	3.01391
N	1.15267	3.10828	3.75646
N	3.46080	-3.34354	2.20290
N	1.71959	-1.56535	-2.05693
N	2.18336	-3.68281	-2.43268
N	5.90328	-4.69629	0.55722

N	-2.18139	-5.39445	-0.12748
N	-0.79235	-1.25252	-0.16001
N	-1.27894	-2.52664	1.56413
N	-5.49422	-4.57076	1.04405
N	-7.35307	3.84404	0.68395
N	-1.42268	1.49078	-1.49673
N	-3.08801	2.67044	-2.31395
N	-5.95003	1.76807	-0.68400
C	2.24898	6.79133	1.44833
C	1.78697	5.58755	-0.60853
C	1.58516	3.14871	-4.50788
C	1.50794	0.94921	-4.28717
C	1.18077	2.82858	-3.23493
C	0.86949	3.76702	-2.10368
C	2.14002	4.43219	-1.53056
C	4.35825	3.47454	-1.35221
C	5.20218	2.27449	-0.94530
C	5.53789	1.69766	2.88487
C	3.19332	2.43175	2.74281
C	0.96500	1.89465	1.61417
C	1.73168	2.04885	2.94297
C	0.95545	2.96963	5.06221
C	0.50481	4.21740	5.80934
C	2.50150	-3.57033	3.27583
C	3.63721	-4.17468	1.17691
C	2.93378	-1.87020	-1.47462
C	1.29342	-2.67761	-2.63350
C	3.24209	-3.19145	-1.68603
C	4.38006	-4.05326	-1.24724
C	4.77267	-3.84011	0.23269
C	7.13673	-4.34462	0.22667
C	8.22582	-5.37785	0.47916
C	-1.11947	-6.38791	-0.03893
C	-3.18255	-5.29755	0.75745
C	-2.14355	-1.52519	-0.17379
C	-0.29648	-1.86953	0.89853
C	-2.47568	-2.31443	0.89811
C	-3.77445	-2.89680	1.33770
C	-4.18587	-4.16662	0.55407
C	-6.22291	-5.46771	0.39223
C	-7.44251	-6.01045	1.12238
C	-8.29523	4.67036	1.43496
C	-6.23891	3.38470	1.23937
C	-2.10834	2.07598	-0.45552
C	-2.02970	1.86829	-2.60824
C	-3.15247	2.82192	-0.93604

C	-4.25001	3.53359	-0.22511
C	-5.30380	2.55324	0.36384
C	-5.85074	0.43890	-0.69033
C	-6.27545	-0.25589	-1.97618
H	2.53894	7.73416	0.97205
H	2.86998	6.62530	2.33125
H	1.19691	6.87937	1.74559
H	3.02669	4.90229	0.84825
H	1.76552	4.09994	-4.98595
H	2.08383	1.82635	-6.11778
H	1.54400	-0.09773	-4.54261
H	0.19953	4.56612	-2.43329
H	0.35416	3.21395	-1.31567
H	2.66261	4.93065	-2.35697
H	2.68666	2.54955	-0.63077
H	5.58647	1.79390	-1.85215
H	4.64430	1.54048	-0.35677
H	6.06467	2.63152	-0.37442
H	5.72404	2.76640	2.77321
H	5.93274	1.17629	2.00524
H	6.04755	1.33141	3.78220
H	3.76368	0.58017	3.25746
H	0.86075	2.88515	1.15440
H	-0.04041	1.53964	1.86636
H	1.64667	1.12891	3.52436
H	1.19174	4.03783	3.35686
H	0.37191	5.09330	5.16549
H	1.24500	4.45114	6.58163
H	-0.44153	4.00113	6.31479
H	1.86858	-4.41180	2.99044
H	1.88830	-2.67643	3.43091
H	3.01351	-3.81418	4.21406
H	4.02278	-2.50338	2.23992
H	3.49158	-1.11959	-0.93372
H	0.35566	-2.77191	-3.16328
H	2.07978	-4.63800	-2.74787
H	4.11095	-5.10830	-1.37172
H	5.27675	-3.86152	-1.84781
H	5.11583	-2.80977	0.36274
H	5.69730	-5.64982	0.83046
H	8.68555	-5.64676	-0.47761
H	7.86557	-6.28877	0.96939
H	9.00375	-4.92251	1.09941
H	-1.27862	-6.96782	0.87093
H	-0.13687	-5.90489	0.00818
H	-1.15112	-7.06366	-0.90154

H	-2.21632	-4.80841	-0.95230
H	-2.78455	-1.13049	-0.94649
H	0.73489	-1.82519	1.21283
H	-1.16201	-3.08841	2.39706
H	-3.73036	-3.14399	2.40752
H	-4.56286	-2.15090	1.19788
H	-4.28820	-3.92236	-0.50717
H	-5.64213	-4.47437	2.04075
H	-7.70551	-5.44057	2.02027
H	-7.24166	-7.04810	1.41202
H	-8.29318	-6.01521	0.43549
H	-7.75264	5.48830	1.91323
H	-8.80481	4.09330	2.21567
H	-9.03386	5.07888	0.74123
H	-7.70326	3.36511	-0.13594
H	-1.82448	1.91584	0.57401
H	-1.75508	1.54021	-3.60360
H	-3.66251	3.14749	-2.99546
H	-3.84695	4.11666	0.60866
H	-4.74759	4.25083	-0.89382
H	-4.80946	1.84058	1.02395
H	-6.11311	2.21885	-1.57649
H	-5.38009	-0.60096	-2.50653
H	-6.85176	0.38638	-2.65177
H	-6.87108	-1.13724	-1.72519

Small Model – SOR-hydroperoxo Active Site

Fe	-0.29268	-0.29658	-0.20542
S	-0.89192	-0.48439	2.09722
O	-0.05475	-0.78985	-3.13888
O	0.03939	0.21463	-2.08792
N	-2.70008	-3.33493	-2.08797
N	-1.26507	-2.19051	-0.86895
N	-2.20587	0.83406	-0.47000
N	-3.56864	2.28794	-1.39894
N	0.74496	1.61043	0.15608
N	1.41604	3.49095	1.07100
N	1.72996	-1.17828	-0.21299
N	3.60710	-1.77005	-1.18937
C	-0.35851	-4.10882	1.69571
C	-0.04532	-0.89741	4.74804
C	-5.79851	2.08061	1.71079
C	2.49817	5.48267	-1.34171
C	5.96996	0.16484	0.08371
C	-1.89598	-4.26459	-1.45739

C	-2.28509	-2.10718	-1.71186
C	-1.00468	-3.55187	-0.69520
C	0.04801	-4.11315	0.21428
C	0.47525	-0.75126	3.31388
C	-3.28834	1.03883	0.37027
C	-2.40510	1.60432	-1.52954
C	-4.15543	1.94406	-0.18877
C	-5.45394	2.52025	0.28478
C	1.74550	2.15678	-0.62520
C	0.56890	2.43694	1.17442
C	2.18721	3.33116	-0.07265
C	3.17191	4.34995	-0.54960
C	2.77719	-0.99534	0.67216
C	2.26470	-1.64937	-1.33007
C	3.96388	-1.35053	0.08473
C	5.38256	-1.18880	0.53043
H	-0.63677	-3.10557	2.02450
H	-1.21960	-4.76631	1.86529
H	0.46741	-4.47138	2.31944
H	-0.59281	-0.00320	5.06534
H	-0.72104	-1.75450	4.83636
H	0.79461	-1.04995	5.43800
H	-5.90101	0.99202	1.77961
H	-5.02744	2.39615	2.42208
H	-6.74829	2.52441	2.02534
H	1.97955	5.08666	-2.22134
H	1.76190	6.01780	-0.73035
H	3.24135	6.21214	-1.68297
H	5.96456	0.26267	-1.00830
H	5.38899	0.99473	0.49958
H	7.00674	0.26678	0.42377
H	0.19366	-0.25263	-3.91169
H	-2.02688	-5.32753	-1.59368
H	-3.45641	-3.53299	-2.72888
H	-2.72141	-1.19272	-2.07862
H	0.25754	-5.14164	-0.10513
H	0.97683	-3.55105	0.09067
H	1.03045	-1.64911	3.02426
H	1.16360	0.10101	3.25106
H	-3.35994	0.53060	1.31943
H	-1.72886	1.68321	-2.36713
H	-3.94030	2.94792	-2.07016
H	-5.40506	3.61791	0.24045
H	-6.26338	2.22318	-0.39797
H	2.06260	1.67041	-1.53469
H	-0.13761	2.29331	1.97907

H	1.48269	4.25651	1.72958
H	3.72923	4.76543	0.30091
H	3.91073	3.84655	-1.18328
H	2.61978	-0.59550	1.66091
H	1.71816	-1.87387	-2.23531
H	4.24060	-2.12218	-1.89577
H	5.41707	-1.26355	1.62301
H	5.99946	-2.01229	0.14706

Large Model – SOR-hydroperoxo Active Site

F e	0.23300	0.07363	-1.52410
S	1.67281	0.73831	0.37797
O	-5.28817	-0.14032	0.16376
O	-5.82217	3.78449	2.31655
O	-5.99786	-5.76890	-0.77260
O	-3.31384	-5.94080	1.76829
O	7.34837	-3.32347	-0.25554
O	2.88490	-5.21572	0.98926
O	1.09179	1.88733	5.62005
O	3.51167	3.53220	2.31809
O	4.90971	4.35456	-1.99242
O	1.01159	6.39585	-1.01856
O	-0.91868	-0.86497	-2.82004
O	-0.94984	-0.41912	-4.19924
N	-5.93229	1.83171	-0.72344
N	-2.94422	2.81210	-2.28783
N	-1.35182	1.55404	-1.45767
N	-7.31571	3.92657	0.63580
N	-5.55173	-4.50774	1.02002
N	-1.30343	-2.58392	1.49106
N	-0.84945	-1.18501	-0.13597
N	-2.24534	-5.37100	-0.14064
N	5.84480	-4.76141	0.56350
N	2.12835	-3.65242	-2.39063
N	1.65925	-1.56015	-1.91747
N	3.41332	-3.37766	2.19976
N	1.17339	3.10294	3.73236
N	4.10543	1.46136	3.00120
N	3.09616	3.36271	-1.09048
N	1.19338	1.35176	-3.04026
N	2.10082	1.77557	-4.99859
N	2.50346	5.64878	0.50919
C	-6.51520	-0.20785	-1.89594
C	-5.84794	0.50165	-0.72691
C	-5.27998	2.61237	0.32395

C	-4.20541	3.58650	-0.23172
C	-3.08826	2.87643	-0.91164
C	-1.89292	2.01232	-2.57744
C	-2.08550	2.08443	-0.41717
C	-6.20816	3.45613	1.19489
C	-8.24477	4.77502	1.38566
C	-7.51409	-5.93030	1.09150
C	-6.28888	-5.39785	0.36870
C	-4.23789	-4.11922	0.53309
C	-3.81783	-2.86313	1.33637
C	-2.51971	-2.27976	0.90157
C	-0.32734	-1.90903	0.84657
C	-2.21149	-1.41098	-0.11213
C	-3.24760	-5.26071	0.74135
C	-1.25367	-6.44078	-0.06930
C	8.16666	-5.45379	0.50891
C	7.08299	-4.42437	0.23556
C	4.72471	-3.89343	0.23433
C	4.33508	-4.07105	-1.24839
C	3.19940	-3.18764	-1.64771
C	1.22852	-2.65531	-2.53284
C	2.89105	-1.87842	-1.37192
C	3.58306	-4.21310	1.17609
C	2.49622	-3.64112	3.30460
C	0.55566	4.22386	5.78901
C	0.97114	2.96993	5.03775
C	1.74267	2.03537	2.92228
C	0.94070	1.91510	1.60280
C	3.20893	2.40159	2.72550
C	5.54944	1.67664	2.96700
C	5.24361	2.24822	-0.89712
C	4.39606	3.42157	-1.36888
C	2.18908	4.40365	-1.55519
C	0.92027	3.74006	-2.13089
C	1.27660	2.73902	-3.19509
C	1.70162	0.81329	-4.14331
C	1.83716	3.00144	-4.41983
C	1.84671	5.56492	-0.63688
C	2.33212	6.78252	1.40843
H	-5.78516	-0.85945	-2.38574
H	-7.31182	-0.85020	-1.50686
H	-6.94531	0.46992	-2.64143
H	-6.27646	2.29575	-1.55447
H	-4.80555	1.88654	0.98364
H	-4.67415	4.30869	-0.91416
H	-3.82491	4.16451	0.61604

H	-3.48665	3.33199	-2.96559
H	-1.56713	1.76932	-3.57692
H	-1.86899	1.84779	0.61284
H	-7.68735	3.44701	-0.17346
H	-8.97500	5.19344	0.68980
H	-8.76326	4.20833	2.16711
H	-7.68669	5.58443	1.85968
H	-8.35136	-5.96786	0.38991
H	-7.30796	-6.95585	1.41861
H	-7.79878	-5.33531	1.96581
H	-5.70012	-4.41208	2.01722
H	-4.33345	-3.86484	-0.52648
H	-4.59843	-2.10825	1.20671
H	-3.77276	-3.12681	2.40152
H	-1.17025	-3.23074	2.25852
H	0.71774	-1.94377	1.11217
H	-2.88056	-0.92581	-0.80322
H	-2.35420	-4.89787	-1.02918
H	-1.55038	-7.30087	-0.68162
H	-0.28160	-6.06796	-0.40531
H	-1.17485	-6.76643	0.96831
H	8.93748	-4.99339	1.13423
H	7.80083	-6.36026	1.00239
H	8.63876	-5.73008	-0.43951
H	5.63138	-5.70997	0.84933
H	5.08289	-2.86897	0.37639
H	5.22911	-3.86157	-1.84597
H	4.05763	-5.11864	-1.40725
H	2.02667	-4.59585	-2.74284
H	0.28370	-2.74039	-3.04567
H	3.45907	-1.14982	-0.81335
H	4.08035	-2.62540	2.31444
H	3.02740	-4.05116	4.17150
H	1.99343	-2.71580	3.60217
H	1.76264	-4.37562	2.96937
H	-0.38176	4.02236	6.31603
H	1.31490	4.44823	6.54537
H	0.42257	5.10016	5.14625
H	1.25615	4.03393	3.34071
H	1.63891	1.11620	3.50264
H	-0.06706	1.58881	1.87485
H	0.86281	2.90629	1.14396
H	3.76810	0.60396	3.41821
H	5.96967	1.62522	3.97736
H	6.03394	0.92580	2.33470
H	5.73388	2.66820	2.55400

H	6.07532	2.63718	-0.30227
H	4.68365	1.51782	-0.30530
H	5.67672	1.75217	-1.77246
H	2.71963	2.54276	-0.61452
H	2.72289	4.89043	-2.38080
H	0.36784	3.24709	-1.33000
H	0.27797	4.53107	-2.52822
H	1.76320	-0.24141	-4.35644
H	2.52943	1.62301	-5.90213
H	2.10254	3.93223	-4.89826
H	3.09835	4.88413	0.81341
H	2.94560	6.61245	2.29542
H	2.64846	7.71074	0.92161
H	1.28176	6.89881	1.69874
H	-1.67152	-0.97358	-4.54622

2. MM parameters (Forces)

Amber files (lib for charges and frcmod for forces) can be downloaded in a zip file as supporting materials.

DX Active Site

Table S1. Force constants and equilibrium values for bond stretching and angle bending for the DX active site.

Bond	Stretching force constant (kcal mol^{-1} $Å^{-2}$)	Equilibrium bond length (Å)
FE-S_{CXXC}	78.18	2.316
FE-S_{CC}	78.17	2.321
CT-S_{CC}	134.01	1.850
CT-S_{CXXC}	135.03	1.850

Angle	Bending force constant (kcal mol^{-1} rad^{-2})	Equilibrium bond angle (°)
S_{CXXC}-FE-S_{CXXC}	25.538	114.754
S_{CXXC}-FE-S_{CC}	29.800	106.336
SCC-FE-S_{CC}	30.695	117.165
CT-S_{CXXC}-FE	59.822	105.053
CT-S_{CC}-FE	56.554	106.056

Fe^{2+}-$OO^{\bullet-}$ **active site**

Table S2. Force constants and equilibrium values for bond stretching and angle bending for the Fe^{2+}-$OO^{\bullet-}$ active site.

Bond	Stretching force constant (kcal mol^{-1} $Å^{-2}$)	Equilibrium bond length (Å)
FE-NB	19.05	2.283
FE-SH	36.21	2.492
OP-FE	25.49	2.206
OP-OD	483.08	1.333

Angle	Bending force constant (kcal mol^{-1} rad^{-2})	Equilibrium bond angle (°)
FE-OP-OD	12.342	124.553
NB-FE-OP	27.567	83.253
SH-FE-OP	20.076	171.109
NB-FE-NB	33.640	114.819
NB-FE-SH	38.609	96.642

Fe^{3+}-OOH **active site**

Table S3. Force constants and equilibrium values for bond stretching and angle bending for the Fe^{3+}-OOH active site.

Bond	Stretching force constant (kcal mol^{-1} $Å^{-2}$)	Equilibrium bond length (Å)
FE-NB	29.07	2.219
FE-SH	51.26	2.387
OP-FE	76.39	1.979
OP-OD	265.48	1.457
OD-OH	553.0	0.960

Angle	Bending force constant (kcal mol^{-1} rad^{-2})	Equilibrium bond angle (°)
FE-OP-OD	35.222	119.823
NB-FE-OP	38.363	85.827
SH-FE-OP	32.731	168.610
NB-FE-NB	40.208	116.828
NB-FE-SH	37.632	94.034
OP-OD-OH	32.737	100.120

II. Results and discussions

1. Validity of the models

Backbone hydrogen bonding analysis were done with the Hydrogen Bonds plugins in the VMD program[1]. Parameters were set to a distance of 3.5 Å for the bonds between two heavy donor-acceptor atoms and 30° for the donor-hydrogen-acceptor angle cutoff.

DX Site. In our calculations, the averaged Fe-S distance over the four bonds is 2.30 ± 0.06 Å, which is in good agreement with the two crystal structures. Indeed, averaged Fe-S distances are 2.27 Å for 2JI3 and 2.29 Å for 1DXG[2] (both averaged over the four Fe-S bonds and the 2 chains). This Fe-S distance also matches the result from the work of Carvalho[2] giving a Fe-S distance of 2.30 ± 0.06 Å. Distinguishing the CC and CXXC sequences for angles, we found 108.3 ± 3.6° and 106.0 ± 3.7° for the Fe-S_{CC}-C and the Fe-S_{CXXC}-C angles respectively. The averaged values obtained from the X-Ray structures are 107.2° and 105.2° for 2JI3 and 107.1° and 103.6° for 1DXG. Carvalho reported values of 109.3 ± 3.4° in the CC motif and 105.4 ± 3.4° in the CXXC. As previously reported, angles Fe-S-C for the vicinal cysteines are slightly greater than the ones for the cysteines separated by two amino acids. Studying the H-bonding network around the sulfur atoms, we can see (values are reported in Table S4) it bears good agreement to the DX H-bonding reported by Archer *et al*[3,4] in his experimental work on *Desulfovibrio gigas* and to the theoretical work of Carvalho *et al*[2]. Despite a different peptide sequence, we found the same H-bonding between sulfurs atoms and the nearby amino acids. For the A chain, there is a H-bond between the amide group of Val^{12} and S_{Cys10}, which is found in the DX from *Desulfovibrio gigas* as an hydrogen bond between Leu^{12} and S_{Cys9}. A bond between Cys^{13} and S_{Cys10} corresponds to a bond between Cys^{12} and S_{Cys9}. Also, there are two H-bonds formed by the

Asn^{15} with the backbone amide towards S_{Cys13}, and the amide from the sidechain towards S_{Cys29} (Equivalent to Gln^{14} towards S_{Cys12} and towards S_{Cys28} respectively). The same goes for the DX active site present in chain B of the SOR.

Table S4. Hydrogen bonds between sulfur atoms of the DX center and amide groups from the chain.

	Acceptor	Donor		Distance H-A (Å)	Distance N-A (Å)	Angle D-H-A (°)
Chain A	S_{CXXC} Cys^{10}	H Val^{12}	N Val^{12}	2.70 ± 0.3	3.55 ± 0.2	144 ± 12
	S_{CXXC} Cys^{10}	H Cys^{13}	N Cys^{13}	2.77 ± 0.4	3.62 ± 0.3	146 ± 19
	S_{CXXC} Cys^{13}	H Asn^{15}	N Asn^{15}	2.77 ± 0.2	3.66 ± 0.2	149 ± 11
	S_{CC} Cys^{29}	HD2 Asn^{15}	ND2 Asn^{15}	2.45 ± 0.4	3.40 ± 0.3	161 ± 13
Chain B	S_{CXXC} Cys^{139}	H Val^{141}	N Val^{141}	2.68 ± 0.3	3.53 ± 0.2	143 ± 13
	S_{CXXC} Cys^{139}	H Cys^{142}	N Cys^{142}	2.74 ± 0.4	3.60 ± 0.3	147 ± 19
	S_{CXXC} Cys^{142}	H Asn^{144}	N Asn^{144}	2.79 ± 0.2	3.68 ± 0.2	149 ± 12
	S_{CC} Cys^{158}	HD2 Asn^{144}	ND2 Asn^{144}	2.48 ± 0.4	3.43 ± 0.3	161 ± 14

Concerning the bonding with water, SCys30 is 50% of the simulation time H-bonded to water molecules with a low residency time (40 ps) because the sulfur is widely accessible to the solvent. For SCys10, the sulfur is at the end of a pocket causing a steric hindrance preventing the free circulation of water molecules. Thus in this case, the average occupancy is only 10% of the time, but contrasted to Cys30, only by a few water molecules, each one staying around 5 ns. The other two sulfur (Cys^{13} and Cys^{29}) atoms are not solvent exposed, and so no H-bonding with water was found.

Fe^{2+}-$OO^{\bullet-}$ site. Two QM models caught our attention. A small one by Sit *et al*[5] (56 atoms, hereafter *small* - C_β histidines & methyl thiolate – gas phase) and a larger one by Tremey *et al*[6] (87 atoms taking into account H-bonding with the sulfur, hereafter *large* - C_α histidines, cysteine & backbone atoms between Cys^{116} and His^{119} (C model) – implicit water). Both models used the B3LYP functional with a DZVP quality basis set. For the Fe-S bond distance, we report values of 2.49 ± 0.1 Å for the A chain and 2.47 ± 0.1 Å for the B chain. For QM calculations, the *small*[5] model reported a value 2.50 Å and the *large*[6], 2.71 Å. For the Fe-Op bond, *small* and *large* QM models gave values of 2.27 Å and 2.20 Å respectively, while we obtained an average value of 2.31 ± 0.11 Å. For the Op-Od bond and the Fe-Op-Od angle, we obtained values of, 1.33 ± 0.0 Å and 136 ± 7°. For QM calculations the *small* model reported 1.34 Å and 128.6° and the *large* model 1.34 Å and 125.5°. This little fluctuation can be explained by the fact that both MM parameters in this work and previous QM models were based on either X-ray structures of the wild type (2JI1 corresponding to Fe^{2+}, *large* model) or of an intermediate (2JI3 corresponding to Fe^{3+}-OOH, this work and *small* model). Nevertheless, we can note that the correlation shown in [6] between the two bonds is still conserved: the shortening of the Fe-S bond in this MM model implies a lengthening of the Fe-Op bond. This trans effect has been shown to be modulated by the presence of a H-bond network around the sulfur atom which affects the Fe-S interaction and in turn affect the properties (geometries, reactivity) of the Fe-OO(H) part[6]. We therefore studied the H-bonding network toward the axial sulfur. In our simulations, the amide groups of the backbone of Ile^{118} and His^{119} make hydrogen bonds with the sulfur at an occupancy rate of 39% and 35%, respectively, for the A chain site. For the B chain site, values of 24% and 62% are found. Lengths and angles are reported in the Table S5.

Table S5. Hydrogen bonds between sulfur atoms of the Fe^{2+}-$OO^{\bullet-}$center and amide groups from the chain.

	Acceptor	Donor		Distance H-A (Å)	Distance N-A (Å)	Angle D-H-A (°)
Chain A	S Cys^{116}	H Ile^{118}	N Ile^{118}	2.21 ± 0.1	3.28 ± 0.1	160 ± 9
	S Cys^{116}	H His^{119}	N His^{119}	2.23 ± 0.1	3.21 ± 0.1	164 ± 10
Chain B	S Cys^{245}	H Ile^{247}	N Ile^{247}	2.27 ± 0.1	3.23 ± 0.1	158 ± 8
	S Cys^{245}	H His^{248}	N His^{248}	2.21 ± 0.1	3.20 ± 0.1	166 ± 9

2. Description of the H-Bonding network around the active site

H-Bonding geometry characteristics and cutoffs. The bond length between one hydrogen atom and one donor heavy atom (nitrogen or oxygen) is set to 1.1 Å. The hydrogen bond length between one hydrogen and one acceptor heavy atom (nitrogen or oxygen) is set to 2.2 Å. The distance between two heavy atoms, donor and acceptor is set to 3.3 Å. The analysis was done in VMD either using the Hydrogen Bonds plugin (referred as "plugin") or by scripting in the tcl/tk console (referred as "our method").

For the "direct" system, our method was used: the oxygen (proximal or distal) must be located within 2.2 Å of a hydrogen (H_{lys}) belonging to the NH_3^+ group of the lysine 48 and within 3.3 Å of the nitrogen (N_{lys}) belonging to the NH_3^+ group of the lysine 48. Also we used the plugin with a distance of 3.3 Å and a cutoff angle of 40°. Both analyses gave the same count of H-Bonding.

For the "one water bridge", our method was used: the oxygen (Op or Od) must be located within 2.2 Å of a hydrogen (Hw_1) belonging to a water molecule and within 3.3 Å of the oxygen

(Ow_1) belonging to the same water molecule (1.1 Å distance between Hw_1 and Ow_1). The Ow_1 must be located within 2.2 Å of a H_{lys} and within 3.3 Å of the N_{lys}.

For the "two water bridge", our method was used: the oxygen (Op or Od) must be located within 2.2 Å of a hydrogen (Hw_1) belonging to a water molecule and within 3.3 Å of the oxygen (Ow_1) belonging to the same water molecule (1.1 Å distance between Hw_1 and Ow_1). The Ow_1 must be located within 2.2 Å of a hydrogen (Hw_2) belonging to another water molecule and within 3.3 Å of the oxygen (Ow_2) belonging to the same water molecule (1.1 Å distance between Hw_2 and Ow_2). The Ow_2 must be located within 2.2 Å of a H_{lys} and within 3.3 Å of the N_{lys}.

Fe^{2+}-$OO^{\bullet-}$ site. The three patterns are represented in Figure S1.

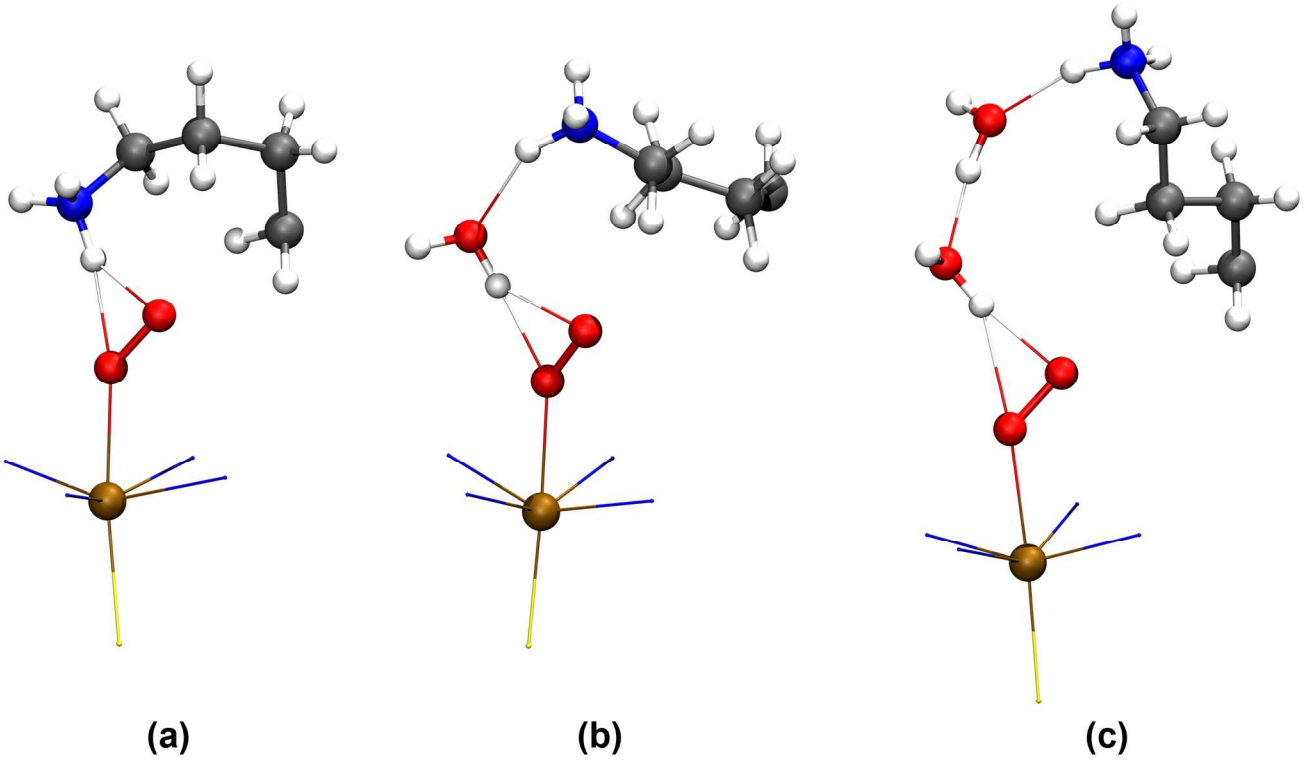

Figure S1. Three configurations for the Fe^{2+}-$OO^{\bullet-}$ site. (a) Lysine directly H-bonded to the superoxide noted as "direct". (b) One water molecule involed in the H-bond network between

lysine and superoxide noted as “one water bridge”. (c) Two interstitial water molecules between the lysine and the superoxide noted as “two water bridge”.

The direct H-bonding pattern is pretty rare, about twenty times less, compared to the two bridged patterns. This direct interaction can be made with both oxygen atoms of the substrate (proximal and distal) but occurs more often with the distal oxygen than with the proximal one. With one or two bridged water molecules, the distal oxygen is also the favored acceptor of the H-bond.

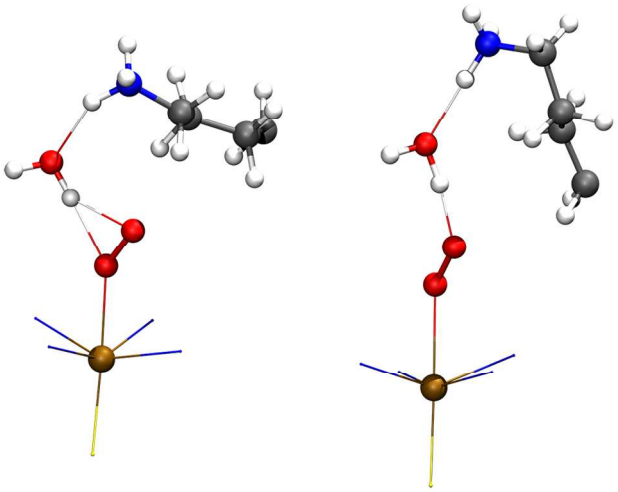

Figure S2. Left: both oxygens are H-bonded by the bridging water. Right: Only the distal oxygen is H-bonded.

It is important to note that when a H-bond is formed with the proximal oxygen, it is also bonded to the distal one (see Figure S2), whereas the opposite is not true: about two third of the distal H-bonding are unique to it. This difference can be explained by the fact the distal is more accessible than the proximal due to steric hindrance. Also the electronic charges (as found by DFT for the MM parameters) are in favor of the distal which is more negative in the superoxide-complex than the proximal. The results are consistent with the distal oxygen will likely be the

first to be protonated to form a hydroperoxide[7–9]. In addition, experimental results tend to show that the Lys[48] has an important (but not essential[6]) role in the first protonation step as the final proton donnor[5]. When Od is involved in a H-bond network, 37% of the configurations imply an interaction with Lys[48], may it be direct or involve water while only 25% of the configurations do not involve lysine. We can also note that the proximal oxygen is more involved in H-bond with water alone (38%) than the distal oxygen (25%). This is assumed to be a direct consequence of the geometry around the active site: Op is more accessible than Od.

3. QM/MM Dynamics

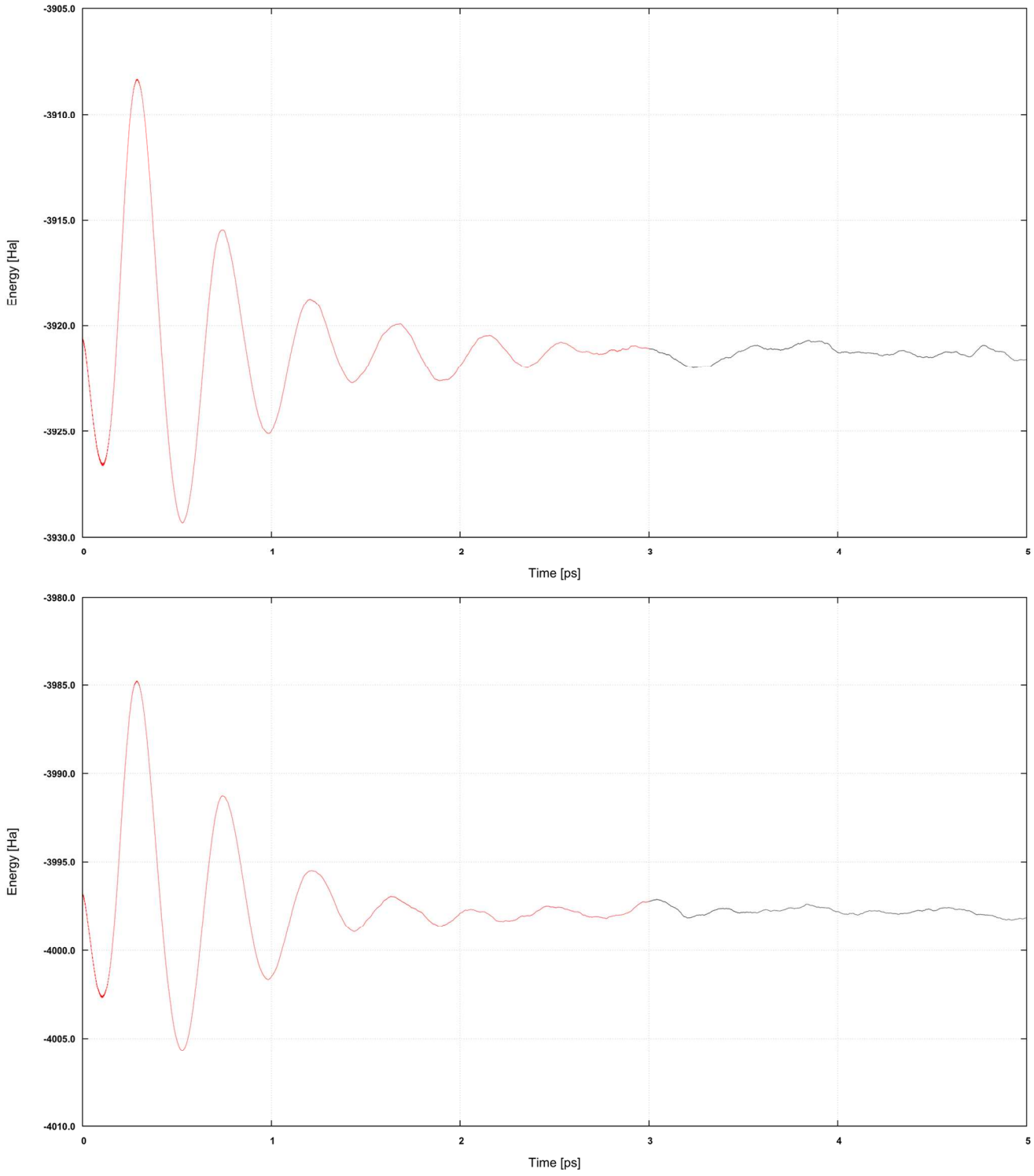

Figure S3. Sum of the QM/MM potential energy and QM/MM kinetic energy of system as a function of simulation time. Top is the direct system, bottom is the 'one water bridge' system.

We can see on Figure S3, the necessity of running an unbiased QM/MM dynamics before biasing the system via metadynamics. The first 3 ps (Fig. S3, in red) show a fluctuation, slowly stabilizing, is the result from the MM to QM/MM transition. The time from 3 ps to 5 ps is the equilibrated part (Fig. S3, in black). Extracted geometrical or electronics values as well as starting metadynamics geometries and velocities will be on this 2 last ps. The active site geometry is well preserved (Table S6).

Table S6. Relevant values of distances and angles (bending and dihedral) for the Fe^{3+}-OOH center from both systems (averaged for the last two 2 ps).

Distance (Å)	Fe-Op	S-Fe	Op-Od	
Direct	1.99 ± 0.05	2.49 ± 0.10	1.45 ± 0.03	
One water bridge	1.96 ± 0.05	2.48 ± 0.08	1.45 ± 0.04	
Angle (°)	Fe-Op-Od	Op-Od-Hd	C_β-S-Op-Od	Fe-Op-Od-Hd
Direct	118 ± 7	104 ± 4	70 ± 16	94 ± 18
One water bridge	116 ± 6	99 ± 5	-40 ± 17	13 ± 14

4. Metadynamics

One CV metadynamics. We run metadynamics on only one CV (the iron-proximal oxygen distance) to accentuate the difference between the two mechanisms. The free energy profile is represented in the figure S4. The rate-limiting barrier for the 'direct' system is 9 kcal mol^{-1} (in black, Fig. S4) and corresponds to the dissociation of the iron-oxygen as shown in the FES with the two CV for the direct system (where it is 7 kcal mol^{-1}). The system then evolves naturally with the protonation of the $^{-}$OOH moiety subsequently formed. Whereas for the 'one water bridge', the rate-limiting barrier the dissociation is as high as 23 kcal mol^{-1} (in red, Fig. S4), compared to 11 kcal mol^{-1} for the protonation (with 2 CVs) which unfavors this mechanism for the 'one water bridge' configuration.

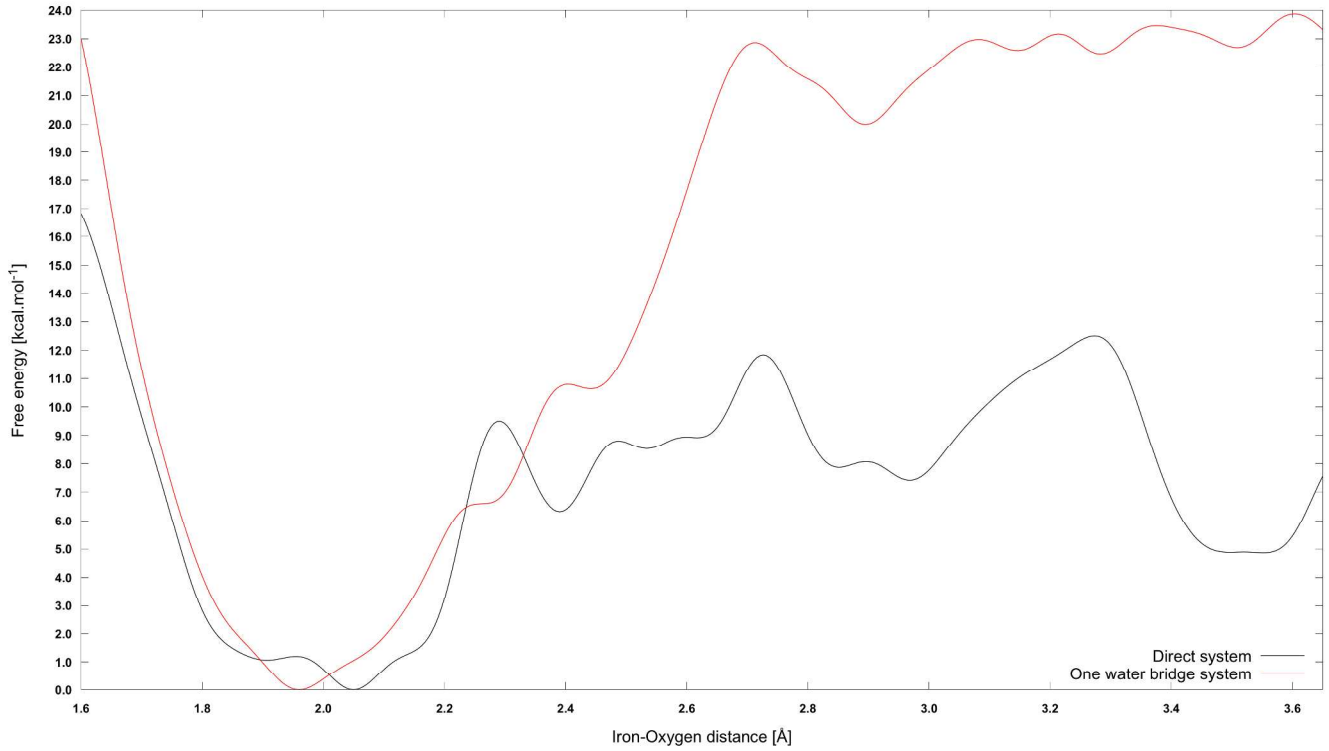

Figure S4. Free energy profile for the Iron-Oxygen distance CV for the 'direct' and the 'one water bridge' systems.

Variations of the CV in function of time for the two metadynamics.

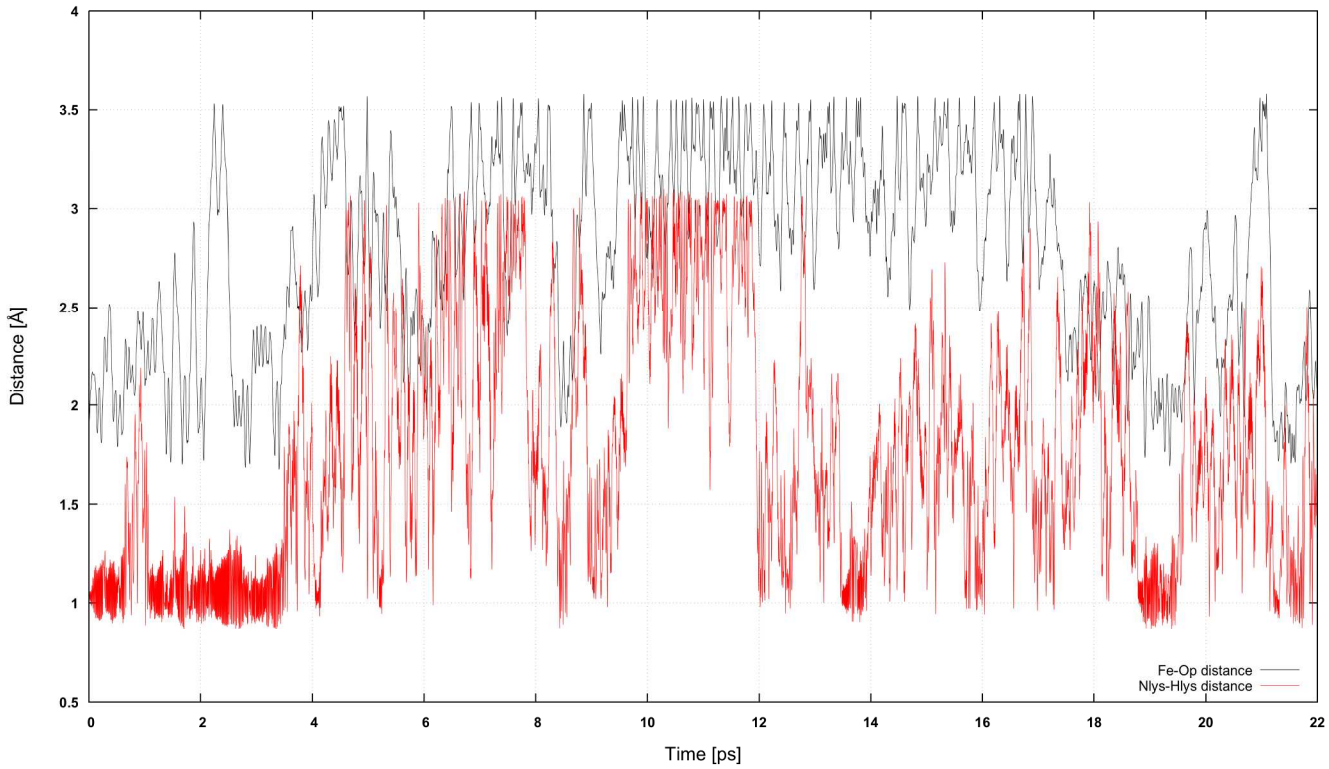

Figure S5. CV as a function of time for the 'direct' conformation metadynamics.

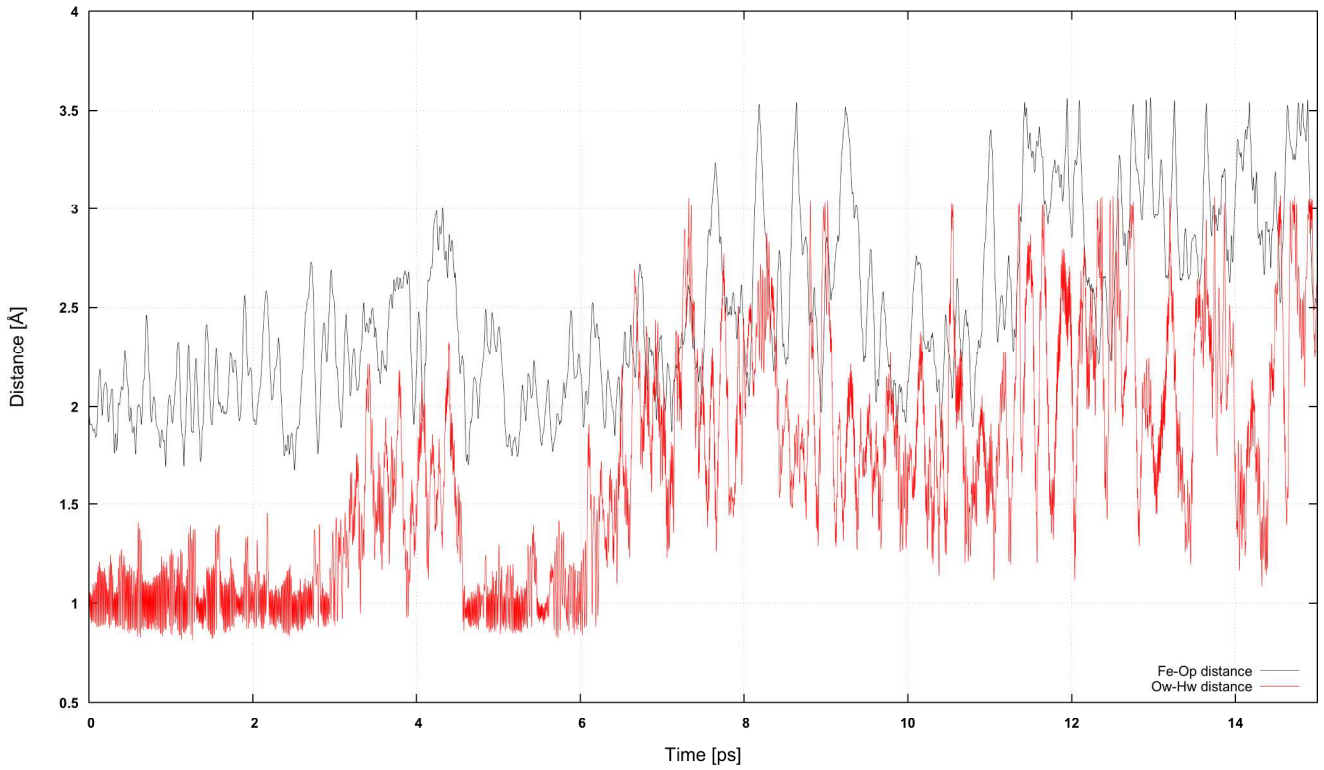

Figure S6. CV as a function of time for the 'one water bridge' conformation metadynamics.

5. Small models analysis

AIM calculations. AIM calculations were performed with the AIMALL 15.09.27 software suite[10] and the Gaussian 09 D 01 program[11]. Following the nomenclature used for the Mulliken population analysis, we performed four calculations: 'direct system', 'direct system' AS with explicit water and lysine, 'one water bridge' AS and 'one water bridge' AS with explicit water and lysine. Values total electronic energy density[12] and delocalization index[13,14] for Fe-Op bond and Op-Od bond can be found in table S7 for the 'direct' system and table S8 for the 'one water bridge'.

Table S7. Values of the total electronic energy density and the delocalization index for the 'direct' system without or with environment. Values extracted from AIMALL software.

	H (Fe-Op bond)	Delocalization Index(Fe,Op) bond	*H* (Op-Od bond)	Delocalization Index(Op,Od) bond
AS	$-1.07\ 10^{-2}$	0.52	$-1.74\ 10^{-1}$	1.24
AS with explicit water and lysine	$-9.21\ 10^{-3}$	0.47	$-1.76\ 10^{-1}$	1.23

Table S8. Values of the total electronic energy density and the delocalization index for the 'one water bridge' system without or with environment. Values extracted from AIMALL software.

	H (Fe-Op bond)	Delocalization Index(Fe,Op) bond	*H* (Op-Od bond)	Delocalization Index(Op,Od) bond
AS	$-1.20\ 10^{-2}$	0.52	$-1.78\ 10^{-1}$	1.23
AS with explicit water and lysine	$-9.76\ 10^{-3}$	0.59	$-1.79\ 10^{-1}$	1.23

For the Op-Od bond, there is no noticeable difference between the two systems with or without environment for both descriptors.

Concerning the Fe-Op bond strength (using total electronic energy density, *H*), there are several variations. Firstly, between the 'direct' system and the 'one water bridge' system, the bond is weaker in the case of the 'direct' system by roughly 10% (either with or without the environment) compared to the 'one water bridge'. Secondly, the Fe-Op bond is also weakened by the environment by roughly 20% (either for the 'direct' and 'one water bridge' system). The delocalization index provides also information regarding that the environment plays a noticeable role: both systems with only the active site account for a DI(Fe,Op) of 0.52 whereas with the environment, the 'direct' system take a value of 0.47 and the 'one water bridge' a value of 0.59. It must be reinforced that the Fe-Op distances are the same between the respective systems with or without environment.

These differences points towards two conclusions: a description of the environment is needed to account for a correct description of the reactivity (because it has a non-negligible impact on the Fe-Op bond). Moreover, the 'direct' system posses a weakened Fe-Op bond. This is on par with the Mulliken charges analysis.

Mulliken charge analysis 'one-water bridge'. Compared to the direct system, the 'one water bridge' system exhibits a different behavior. The distal oxygen for the AS model is more negative. The geometry on the active site has an impact on the charge distribution (Table S9). Completing the model by adding either the lysine, the bridging water or explicit water or all of them equilibrate the charge (in a 0.10 order) between the two oxygens.

Table S9. Values of the Mulliken charges for both hydroperoxide oxygens in the 'one water bridge' configuration for various models in gas phase. Values extracted from CP2K software

	AS	AS with lysine	AS with explicit water	AS with bridging water	AS with bridging water and lysine	AS with explicit water and lysine	Full system QM/MM
q_{Op} (Proximal oxygen)	-0.40	-0.47	-0.54	-0.55	-0.57	-0.58	-0.55
q_{Od} (Distal oxygen)	-0.49	-0.45	-0.57	-0.48	-0.43	-0.50	-0.50

III. References

(1) Humphrey, W.; Dalke, A.; Schulten, K. {VMD} -- {V}isual {M}olecular {D}ynamics. *J. Mol. Graph.* **1996**, *14*, 33–38.

(2) Carvalho, A. T. P.; Teixeira, A. F. S.; Ramos, M. J. Parameters for Molecular Dynamics Simulations of Iron-Sulfur Proteins. *J. Comput. Chem.* **2013**, *34* (18), 1540–1548.

(3) Archer, M.; Huber, R.; Tavares, P.; Moura, I.; Moura, J. J. G.; Carrondo, M. A.; Sieker, L. C.; LeGall, J.; Romão, M. J.; Romco, M. J. Crystal Structure of Desulforedoxin from Desulfovibrio Gigas Determined at 1.8 A Resolution: A Novel Non-Heme Iron Protein Structure. *J. Mol. Biol.* **1995**, *251* (5), 690–702.

(4) Archer, M.; Carvalho, A. L.; Teixeira, S.; Moura, I.; Moura, J. J. G.; Rusnak, F.; Romão, M. J. Structural Studies by X-Ray Diffraction on Metal Substituted Desulforedoxin, a Rubredoxin-Type Protein. *Protein Sci.* **1999**, *8* (7), 1536–1545.

(5) Sit, P. H.-L.; Migliore, A.; Ho, M.-H.; Klein, M. L. Quantum Mechanical and Quantum Mechanical/Molecular Mechanical Studies of the Iron−Dioxygen Intermediates and Proton Transfer in Superoxide Reductase. *J. Chem. Theory Comput.* **2010**, *6* (9), 2896–2909.

(6) Tremey, E.; Bonnot, F.; Moreau, Y.; Berthomieu, C.; Desbois, A.; Favaudon, V.; Blondin, G.; Houée-Levin, C.; Nivière, V. Hydrogen Bonding to the Cysteine Ligand of Superoxide Reductase: Acid-Base Control of the Reaction Intermediates. *J. Biol. Inorg. Chem.* **2013**, *18* (7), 815–830.

(7) Katona, G.; Carpentier, P.; Niviere, V.; Amara, P.; Adam, V.; Ohana, J.; Tsanov, N.; Bourgeois, D. Raman-Assisted Crystallography Reveals End-On Peroxide Intermediates in a Nonheme Iron Enzyme. *Science (80-.).* **2007**, *316* (5823), 449–453.

(8) Silaghi-Dumitrescu, R.; Silaghi-Dumitrescu, I.; Coulter, E. D.; Kurtz, D. M. Computational Study of the Non-Heme Iron Active Site in Superoxide Reductase and Its Reaction with Superoxide. *Inorg. Chem.* **2003**, *42* (2), 446–456.

(9) Kitagawa, T.; Dey, A.; Lugo-Mas, P.; Benedict, J. B.; Kaminsky, W.; Solomon, E.; Kovacs, J. A. A Functional Model for the Cysteinate-Ligated Non-Heme Iron Enzyme Superoxide Reductase (SOR). *J. Am. Chem. Soc.* **2006**, *128* (45), 14448–14449.

(10) Keith, T. A. AIMAll (15.09.27). TK Gristmill Software, Overland Park KS 2015.

(11) Frisch, M. J.; Trucks, G. W.; Schlegel, H. B.; Scuseria, G. E.; Robb, M. A.; Cheeseman, J. R.; Scalmani, G.; Barone, V.; Mennucci, B.; Petersson, G. A.; Nakatsuji, H.; Caricato, M.; Li, X.; Hratchian, H. P.; Izmaylov, A. F.; Bloino, J.; Zheng, G.; Sonnenberg, J. L.; Hada, M.; Ehara, M.; Toyota, K.; Fukuda, R.; Hasegawa, J.; Ishida, M.; Nakajima, T.; Honda, Y.; Kitao, O.; Nakai, H.; Vreven, T.; Montgomery, J. A., J.; Peralta, J. E.; Ogliaro, F.; Bearpark, M.; Heyd, J. J.; Brothers, E.; Kudin, K. N.; Staroverov, V. N.; Kobayashi, R.; Normand, J.; Raghavachari, K.; Rendell, A.; Burant, J. C.; Iyengar, S. S.; Tomasi, J.; Cossi, M.; Rega, N.; Millam, J. M.; Klene, M.; Knox, J. E.; Cross, J. B.; Bakken, V.; Adamo, C.; Jaramillo, J.; Gomperts, R.; Stratmann, R. E.; Yazyev, O.; Austin, A. J.; Cammi, R.; Pomelli, C.; Ochterski, J. W.; Martin, R. L.; Morokuma, K.; Zakrzewski, V. G.; Voth, G. A.; Salvador, P.; Dannenberg, J. J.; Dapprich, S.; Daniels, A. D.; Farkas, Ö.; Foresman, J. B.; Ortiz, J. V.; Cioslowski, J.; Fox, D. J. Gaussian 09 Revision D.01. Gaussian Inc. Wallingford CT 2009.

(12) Cremer, D.; Kraka, E. Chemical Bonds without Bonding Electron Density- Does the

Difference Electron-Density Analysis Suffice for a Description of the Chemical Bond? *Angew. Chemie Int. Ed.* **1984**, *41* (8), 627–628.
(13) Bader, R. F. W.; Stephens, M. E. Spatial Localization of the Electronic Pair and Number Distributions in Molecules. *J. Am. Chem. Soc.* **1975**, *97* (26), 7391–7399.
(14) Fradera, X.; Austen, M. A.; Bader, R. F. W. The Lewis Model and Beyond. *J. Phys. Chem. A* **1999**, *103* (2), 304–314.